Oxygen vacancy and EC – 1 eV electron trap in ZnO

Gauthier Chicot, Pierre R. Muret, Jean-Louis Santailler, Guy Feuillet, Julien Pernot

Oxygen vacancy and $E_C - 1$ eV electron trap in ZnO

Gauthier CHICOT [1,2], Pierre MURET [1,2], Jean-Louis SANTAILLER[3], Guy FEUILLET[3], and Julien PERNOT [1,2,4]

[1] *Univ. Grenoble Alpes, Inst NEEL, F-38042 Grenoble, France*

[2] *CNRS, Inst NEEL, F-38042 Grenoble, France*

[3] *CEA-LETI, Minatec Campus, 17 rue des Martyrs, 38054 Grenoble Cedex 9, France*[*] *and*

[4] *Institut Universitaire de France, 103 boulevard Saint-Michel, F-75005 Paris, France*

Abstract

Fourier transform deep level transient spectroscopy has been performed between 80 K and 550 K in five $n-$type ZnO samples grown by different techniques. The capture cross section and ionization energy of four electron traps have been deduced from Arrhenius diagrams. A trap 1 eV below the conduction band edge is systematically observed in the five samples with a large apparent capture cross section for electrons ($1.6 \pm 0.4 \times 10^{-13}$ cm^2) indicating a donor character. The assignment of this deep level to the oxygen vacancy is discussed on the basis of available theoretical predictions.

[*] julien.pernot@neel.cnrs.fr

I. INTRODUCTION

ZnO is a very attractive semiconductor for optoelectronic uses. Its direct wide band gap (3.37 eV) and large binding exciton energy (60 meV) allow ZnO to compete with GaN for light emitting diode (LED) applications in the UV spectrum. To fabricate LED devices, the n- and $p-$doping processes must be fully mastered in order to control the conductivity and type of the active layers. Shallow donor levels responsible for the residual n-type conductivity of as-grown materials are commonly attributed to native point defects, hydrogen or III elements (like Al, Ga or In) of the periodic table. Formerly, the oxygen vacancy was believed to be one of these shallow states. However, recent theoretical works indicated that the oxygen vacancy (V_O) is not a shallow donor level but a deep donor level with a negative U behavior and a (2+/0) charge transition in the energy range 1-2 eV below the conduction band edge E_C [1–6]. Based on considerations about the V_O formation energy, some authors found that the concentration of this defect should be low in as-grown $n-$type materials [1, 3], as confirmed by Electron Paramagnetic Resonance (EPR) experiment in which V_O is detected only after irradiation treatment. The goal of this work is to detect the V_O in $n-$type ZnO crystals grown by different techniques, one of which being implanted, using Fourier transform deep level transient spectroscopy (FT-DLTS) technique performed in a wide temperature range (80 K-550 K). Indeed, FT-DLTS is a well adapted technique because its sensitivity is at least one part per thousand of the background doping concentration, thus allowing the detection of trap concentrations as low as 10^{13} cm^{-3}.

This article is organized as follows. In a first part, the experimental details and the FT-DLTS spectra of the five samples grown by different techniques are described. In a second part, the Arrhenius diagrams are analyzed. Finally, the properties of the deepest trap at $E_C - 1$ eV are discussed and an assignment to one of the electronic transitions taking place in the oxygen vacancy is shown to be plausible.

II. EXPERIMENTAL DETAILS

Five $(000\bar{1})$ oriented bulk ZnO samples were investigated in this work : sample #1 is grown by Chemical assisted Vapour phase Transport (CVT) on a ZnO substrate, sample #2 is a CVT crystal grown on sapphire, samples #3 and #4 are HydroThermal (HT) ZnO

crystals and sample #5 is a HT Nitrogen implanted one. Sample #1 is 700 m thick while samples #3, #4 and #5 are 500 μm thick. Sample #2 is an around 700 μm slice cut out from a 7700 μm thick crystal grown on sapphire. Each face of this slice was then chemically and mechanically polished to remove the damaged subsurface and to ensure a good surface quality. In case of sample #1, the polarity face was identified prior to the growth by using diluted HCl etching (O-face is much more sensitive than Zn-face) and/or by measuring the abrasion rate during the polishing process (two times higher in case of O-face by comparison with Zn face). In case of sample #2 , a thin ZnO layer grown by organo-metallic vapor phase epitaxy onto a sapphire wafer composes the seed. The polarity of this template seed is Zn (confirmed par TEM and by chemical etching). In case of samples #3 , #4 and #5, the substrate supplier indicated the face polarity, which has been checked by ourselves. The samples #1 and #2 were grown at 1030 °C [7] and then annealed at 1100 °C during one hour. The HT samples #3, #4 and #5 were annealed at 1100 °C. Then, the sample #5 was implanted with Nitrogen atoms (multi-implantation with energy ranging between 50 and 200 keV and a total dose of 2.2×10^{15} cm^{-2}) and post-annealed at 900°C. The characteristics of the five samples are summarized in Table I. All the samples were cleaned with organic solvents before being treated by Remote Oxygen Plasma (ROP). Pt Schottky contacts (50 nm thick and 500 μm in diameter) were evaporated on the O face of the five samples and full sheet Ti/Au ohmic contacts (20 nm/80 nm) were evaporated on the whole Zn face in order to fabricate the ohmic contact of the diodes.

Capacitance voltage C(V) and deep level transient spectroscopy measurements were performed with Phystech FT1030 hardware and software. The internal bridge operates at 1 MHz, a measurement frequency which has been checked to be lower than the cut-off frequency of all the diodes. FT-DLTS spectra were obtained from the fast Fourier transform (FFT) of the capacitive transients [8], delivering up to 28 Fourier coefficients for each time window. Current voltage (I(V)) measurements were firstly achieved to check the rectifying behavior of Pt contacts and the leakage current at different temperatures. C(V) measurements were then performed using reverse bias voltage to determine the effective doping level $N_d - N_a$. Finally, FT-DLTS analysis were performed between 80 K and 550 K using reverse bias U_r = -2 V for sample #1 #2 #4 #5, U_r =-4 V for sample #3 and a pulse voltage (U_p) of 0 V for all the samples. For the five samples, different times windows (T_w) ranging between 1 ms and 1 s were used in order to collect numerous data, thus improving the accuracy of

the Arrhenius diagram.

III. RESULTS, ANALYSIS AND DISCUSSION

A. Fourier transform deep level transient spectroscopy

A total of seventeen electron traps have been detected in the five samples. Typical FT-DLTS spectra are shown on Fig. 1. The Arrhenius diagrams shown in Fig. 2 were obtained by extracting both temperature and emission rates from the maxima detected in DLTS spectra using up to 28 distinct and independent correlation functions yielding back as much Fourier coefficients. Letter labels have been assigned to the thirteen traps found in these five samples(from a to m). Four additional traps are indicated by a star on the figure Fig. 1 and not reported on Fig. 2. These traps will not be discussed in this article. By linear fitting, the activation energy (from the slope) and the apparent capture cross section (from the ordinate at zero abscissa) have been determined using the standard emission rate formula :

$$e_n = \gamma_n \sigma_n v_{th} N_C \exp\left(\frac{-E_{an}}{kT}\right) \tag{1}$$

where e_n is the emission rate, γ_n the entropy factor assumed to be unity in this section, σ_n the capture cross section, v_{th} the thermal velocity of electrons, N_C the effective density of states in the conduction band, E_{an} the activation energy, k the Boltzmann constant and T the temperature.

Data falling on the same lines in the Arrhenius diagram of Fig. 2 can be grouped into three ensembles of electron traps ((e,f), (g,h) and (i,j,k,l,m)) labelled [EX], where X is their activation energy in meV. The fact that the emission time constant of each ensemble are superimposed on the Arrhenius diagram strongly suggests that each of [E500], [E640] and [E1000] is related to a trap with the same physical origin and common to several samples.

The [E280] trap is only observed in sample #4 and commonly labelled E3 as reported in literature [9]. The electronic properties (activation energy (E_{an}) and apparent capture cross section (σ_n)) of the four electron traps [E280], [E500], [E640] and [E1000] are summarized in Table II. A unique fit has been done for each one using the data from the different samples. It must be noticed that the numerous experimental data due to *i*) the Deep Level Transient Fourier Spectroscopy technique, and to *ii*) the number of samples, involve very weak error bars in the quantities extracted from the fit, irrespective of systematic errors

discussed further. Three traps (a, b and c) with activation energies from 135 meV to 171 meV and rather low capture cross sections (from 5.3×10^{-18} cm^2 to 4.0×10^{-17} cm^2) has been observed in sample #1, #4 and #2. Some works [10–14] mentioned levels with such low energy but larger capture cross sections except in [15, 16]. The trap [E500] observed in sample #2 and #4 is often reported in literature [17–21] and commonly named E4 even if its attribution is still unclear. The trap [E640] has been observed only in samples #1 and #2, which are two CVT grown samples. This correlation with the preparation method probably means that this trap is linked to a specific impurity of the CVT process. In literature [15, 22], the rare possible occurrences of this trap are also reported in CVT samples.

The deepest [E1000] electron trap is systematically observed in the five samples. Since all the samples have been treated by a O plasma, the possibility to introduce such defect by this treatment have been considered. However, the depths investigated below the Schottky contact (see Table III) are too large to be affected by this treatment which is not at the origin of the traps observed in this work. The [E1000] activation energy and apparent capture cross section have been determined by doing a unique and simultaneous fit of experimental data from samples $\#1-3$ and #5. The E_{an} and σ_n values deduced from the Arrhenius diagram have been then used to simulate the FT-DLTS spectra shown in figure 1 (b), both obtained from the first real Fourier coefficient [8]. For the extraction of E_{an} and σ_n values of the [E1000] trap, data coming from the sample #4 were not taken into account. As it is shown in figure 1, the peak of the [E1000] level of sample #4 is rather broad and probably contains the contribution of other levels, so that the relationship between the emission rate and the peak position of the FT-DLTS spectra becomes inaccurate.

For the four other samples, the good agreement between the experimental spectrum and the simulated one, *i*) confirms the confidence given by the error bars and *ii*) indicates that the [E1000] trap is a simple point defect in contrast to extended defects which generally result in more broadened spectra with respect to the Fourier transform of a purely exponential transient [23]. The existence of this trap in the five samples, whatever the growth technique and set-up, suggests a native defect (like interstitial, vacancy and related complexes) rather than a foreign impurity, which would have hardly to be common to all these samples, as the origin of this level. The huge capture cross section ($\sigma_n = 1.6 \pm 0.4 \times 10^{-13}$ cm^2) deduced in this work clearly indicates that the [E1000] trap is attractive for electrons and related to a positive charged centre, and therefore to a donor level. The [E1000] trap densities deduced

from the amplitude of the capacitance transient for each sample (see Table III) demonstrate that the trap concentration is higher in the implanted sample #5 than in other samples. In samples #1, #2, #3 and #4, a concentration of native defects like oxygen vacancy V_O close to a few 10^{14} cm^{-3} may be the equilibrium one after growth and annealing, whereas it is well known that the implantation process is able to create more vacancies, which cannot be completely annealed out. When passing from sample #4 to #5 (same samples but #5 has been implanted), the concentration of [E1000] was multiplied by a factor of more than 30, and the corresponding peak clearly emerges out of the corresponding broad band in sample #4 as shown in Fig. 1 (b). Since the oxygen vacancy V_O is the only deep donor in this ionization energy range with a negative U behavior and a (2+/0) charge transition [1–6], its properties are discussed more deeply in the next section.

B. Electron emission from the oxygen vacancy V_O

Among native point defects, the oxygen vacancy V_O is the only centre which shows thermodynamic transition levels calculated by *ab initio* methods in the upper half of the band gap in most studies [1–4]. An other team of theorists [5, 6] found these transition levels in the lower half of the band gap, although all these authors agree both about the a_1 symmetry of the V_O states, mainly coming from the 4s dangling bonds of the four Zn neighbors which have essentially a conduction band character, and the double donor nature of V_O with a negative correlation energy, making V_O^{2+} and V_O^0 the only stable states. The half of the two electrons transition energy $(E_C - E_T^{2,0})$ (where the upper index holds for the numbers of trapped electrons before and after the transition) is close to 1.2 eV in the studies published by the former authors [1–4]. When the Fermi level is between the one electron transition energies $(E_C - E_T^{1,0})$ and $(E_C - E_T^{2,1})$, the formation energy of V_O^{1+} is always higher than those of V_O^0 and V_O^{2+}, thus making V_O^{1+} unstable. In FT-DLTS, after the capture process resulting from the pulse voltage which makes the trap neutral, since the electron involved in the first ionization is bound more strongly than the second one, the second electron emission follows immediately the first one at a given temperature, resulting in a single peak in the DLTS signature with an amplitude multiplied by two [24]. Therefore, the single thermal activation energy E_{an} measured in FT-DLTS, which is due to a single electron emission from V_O^0 may be determined by $(E_C - E_T^{2,1})$, which is larger than $(E_C - E_T^{1,0})$, the

remaining electron being consequently emitted much faster. The situation was different for the initial and final charge states of defects with negative correlation energy previously known in other semiconductors, because they were either amphoteric in Si [24] or double acceptors lying close to the conduction band in 4H-SiC [25], or double donors lying close to the valence band in Si [24]. Hence, a detailed analysis of the capture cross section derivation and theoretical calculations already published has to be addressed because it can be helpful to either validate or discard the assignment of the present [E1000] level to V_O.

1. *Electron emission related to the $V_O^{0/1+}$ and $V_O^{1+/2+}$ transitions*

Taking both capture and emission kinetics and semiconductor statistics into account, the emission rates of the two transitions at thermodynamic equilibrium can be expressed respectively as

$$e_{n2} = \gamma_1 \sigma_{n1} v_{thn} N_C \exp(-\Delta H_T^{2,1}/kT) \tag{2}$$

for the $V_O^{0/1+}$ transition and

$$e_{n1} = \gamma_0 \sigma_{n0} v_{thn} N_C \exp(-\Delta H_T^{1,0}/kT) \tag{3}$$

for the $V_O^{1+/2+}$ transition, where $\sigma_{n,i}$ is the capture cross section, γ_i the entropy factor discussed in the following, $\Delta H_T^{i+1,i}$ the enthalpy of the transition, i the number of trapped electrons, with $i = 0$ in the case of V_O^{2+}. The entropy factor γ_i has two contributions: the degeneracy factor and the vibrational entropy. The neutral state V_O^0 is obtained if four electrons lie in the four a_1 states, with a total degeneracy of $m = 8$. Consequently, the configuration parts of the degeneracy factor, equal to the ratio of the number of possible combinations $C_m^{i+3}/C_m^{i+2} = \frac{m-i-2}{i+3}$ are respectively 5/4 for σ_{n1} and 2 for σ_{n0}. The other part $\exp(\Delta S_{i,vibr}/k)$ of the entropy factor is due to vibrational entropy which reaches its maximum for band to band transitions and determines the temperature dependance dE_G/dT of the band gap energy E_G [26, 27]. From measurements of Rai and co-workers [28], dE_G/dT is close to 0.1 meV/K in the range 300-450 K, a value which induces upper limits of 1.25 for $\Delta S_{E_G,vibr}/k$ and 3.5 for $\exp(\Delta S_{E_G,vibr}/k)$. But the effective entropy change in the transition $\Delta S_{i,vibr}$ is much smaller because the levels are expected to follow the conduction band edge from which the states of V_O originate and the transition energy is close to only one third of

the band gap energy E_G. Therefore, the total entropy factors γ_0 and γ_1 would be very close to one, as previously assumed.

2. *Capture cross section of the $V_O^{0/1+}$ and $V_O^{1+/2+}$ transitions*

In equations 2 and 3, the capture cross sections σ_{n1} and σ_{n0} are dependent on the microscopic properties of the defect or impurity, and temperature in the general case. Extensive theoretical calculations of the multi-phonons mediated transition probability per unit time and capture cross section of deep levels have been performed within the framework of the Born-Oppenheimer approximation from the seventies to the nineties [29–35]. These quantities are dependent on the average phonon energy $\hbar\omega_q$ in a relative way because $\hbar\omega_q$ has to be compared to the thermal energy kT, to the ionization enthalpy $\Delta H_T^{i+1,i} = p_i\hbar\omega_q$ thus defining the number of phonons p_i necessary for energy conservation and to the Condon shift $S_i\hbar\omega_q$ where the Huang and Rhys factor S_i scales the coupling between the phonon modes and the one electron states. The picture which emerged from these calculations allows to write the capture cross section as:

$$\sigma_{ni} = \sigma_{\infty,i}\ F(\hbar\omega_q/kT, p_i, S_i)\ C_Z \tag{4}$$

where $\sigma_{\infty,i}$ is the capture cross section limit for infinite temperature of a neutral center which directly depends on the matrix element of the non-adiabatic hamiltonian between initial and final states, $F(\hbar\omega_q/kT, p_i, S_i)$ the line shape function of the optical spectrum for a zero photon energy and C_Z the averaged Sommerfeld factor, which takes into account the deformation of the wave functions induced by the Coulomb potential [29, 34]. From the analytic expression given in reference [32], the product $F(\hbar\omega_q/kT, p_i, S_i)\ C_Z$ can be calculated and a thermal activation of the cross section can be inferred. For the oxygen vacancy in ZnO, the Huang and Rhys parameter can be assessed from the configuration diagram given in the Fig. 3 of ref. [1]: close to $p_1/2$ in the transition $\mathrm{V_O^{1+/0}}$ which involves the σ_{n1} capture cross section measured in DLTS experiments and close to p_0 in the transition $\mathrm{V_O^{2+/1+}}$. Generally speaking, the prefactor $\sigma_{\infty,i}$ is more difficult to assess because it is proportional to the matrix elements of the perturbative hamiltonian. It has been estimated in the range $10^{-15} - 10^{-14}$ cm^2 by Henry and Lang [31] for most impurities and is taken to be 10^{-14} cm^2 by Pässler [29]. But as shown by Ridley [30], it is both proportional to

S_i^2 and then increases with the electron-phonon coupling, which is rather high in V_O since S_i are of same magnitude as p_i or $p_i/2$, and to the matrix element of the perturbative hamiltonian calculated by an integral over spatial coordinates of the wave functions of the bound electron and delocalized one. In the case of a vacancy, the wave function of the bound electron spreads over a much larger distance than for an impurity center because it is localized in the dangling bonds of the neighbouring atoms. This fact justifies that $\sigma_{\infty,1}$ must amount to about 2×10^{-13} cm^2 in order to fit the experimental value. The capture cross section σ_{n0} involved in the transition $V_O^{2+/1+}$ is expected to be even greater because the Huang and Rhys parameter S_0 and Z=2 are both higher than in the $V_O^{1+/0}$ transition.

C. Discussion

The emission rate inequality $e_{n2} \ll e_{n1}$ is confirmed both because $\sigma_{n1} < \sigma_{n0}$ and $\Delta H_T^{2,1} > \Delta H_T^{1,0}$, implying that only the slower (e_{n2}) emission events are detected in DLTS at all temperatures. This means that the electronic transition of the oxygen vacancy measured by DLTS is only characteristic to the $V_O^{0/1+}$ transition. Also, the capture cross section of the transition must correspond to a single positively charged center and the activation energy E_{an} deduced from the Arrhenius diagram must be compared to the (0/+) transition calculated by *ab initio* methods.

It must be noticed that the capture cross section which is deduced from an Arrhenius diagram, is neither the effective one in the measurement temperature range nor the theoretical value $\sigma_{\infty,i}$ at infinite temperature but an intermediate value obtained at the intercept of the tangent to the curve with the vertical axis located at infinite temperature. Consequently, in the case of $\sigma_{\infty,1}$, the effective capture cross section in the temperature range of measurements is smaller but still in the range of the value given by the Arrhenius diagram due to the thermal activation of the $F(\hbar\omega_q/kT, p_i, S_i)\ C_Z$ factor. Despite such a lowering, the real capture cross section cannot be measured directly because, taking into account the net doping concentrations given in table I, the typical capture kinetic amounts to only some picoseconds (too short for measurement). Anyway, the order of magnitude of the capture cross section ($\gtrsim 10^{-13}$ cm^2) of the trap measured in this work is in good agreement with a positively charged center (attractive for electron) like the V_O^+ which is the only native defect being related to an electronic state within the band gap with an attractive character for

electrons in ZnO.

The measured activation energy are weaker than those calculated in previously quoted theoretical studies [1–4] by some tenths of eV for the $V_O^{1+/0}$ transition [36]. But both because the systematic presence of the [E1000] trap implies an assignment to a native defect rather than an impurity and the oxygen vacancy is the only native defect which is an attractive centre for electrons, an 1 eV value assigned to the enthalpy of the $V_O^{1+/0}$ transition of the oxygen vacancy is most probable. Moreover, the discrepancy between experimental and most of theoretical transition enthalpies [1–4] is noticeably smaller in comparison with Hofmann *et al.* proposal [37] which assigned the electron trap at $E_C - 530$ meV to the oxygen vacancy. It must be noticed that the assignment of the level at $E_C - 530$ meV to the oxygen vacancy is discarded by two important results reported in this work: *i*) this level is found here ([E500]) in only two of the five samples studied in this work which is inconsistent with a native point defect like the oxygen vacancy, *ii*) this level is found in sample #4 (not implanted) and not in sample #5 (same than #4 but implanted in the case of #5), in contradiction with the assignment to an oxygen vacancy created by implantation process.

The energy level reported by Quemener *et al.* [21] for the E5 trap is in good agreement with our results and seems to be also the V_O, except that the capture cross section is slightly lower. Unfortunately, the Arrhenius diagram has not been shown, preventing the detailed comparison with the five Arrhenius diagrams reported in the present work. Future works will be needed to confirm the assignment of the $V_O^{1+/0}$ to the [E1000] trap. Indeed, the possibility that the [E1000] trap is related to a complex between an impurity (present in ZnO whatever the growth method, most probably H) and a native defect (created by implantation for example) cannot be completely discarded. However, the good agreement between the experimental data reported here for all the five different samples which permitted DLTS measurements up to 450 K and the *ab initio* calculations makes the oxygen vacancy the best candidate for the [E1000] trap.

IV. CONCLUSIONS

Traps have been detected and their parameters extracted from FT-DLTS data in five different $n-$ZnO samples. A salient feature of this work consisted to show that only the deepest level ever detected by an electrical method, labelled [E1000], with a ionization en-

ergy of 1 eV for electrons and a very probable donor character due to its very large capture cross section, turns out to be present in all the five samples, in contrast to other deep levels. From a detailed analysis of the electronic properties of the multi-phonons mediated transitions taking place in the oxygen vacancy and comparison with our experimental results, we can conclude that the capture cross section and ionization energy deduced from the experimental Arrhenius diagram are compatible with those estimated from theoretical considerations pertaining to the oxygen vacancy in ZnO, which is recognized as a double donor with a negative correlation energy.

ACKNOWLEDGMENTS

The authors are grateful to Michel Lannoo for valuable discussions.

---

[1] Janotti A and Van de Walle CG 2005 *Appl. Phys. Lett.* **87** 122102.

[2] Erhart P, Albe K, and Klein A 2006 *Phys. Rev. B* **73** 205203

[3] Janotti A and Van de Walle CG 2007 *Phys. Rev. B* **76** 165202

[4] Oba F, Togo A, Tanaka I, Paier J, and Kresse G 2008 *Phys. Rev. B* **77** 245202

[5] Lany S and Zunger A 2005 *Phys. Rev. B* **72**, 035215

[6] Lany S and Zunger A 2010 *Phys. Rev. B* **81**, 205209

[7] Santailler JL, Audoin C, Chichignoud G, Obrecht R, Kaouache B, Marotel P, Pelenc D, Brochen S, Merlin J, Bisotto I, Granier C, Feuillet G and Levy F 2010 *J. Crystal Growth* **312**, 3417

[8] Weiss S and Kassing R 1988 *Solid-State Electron.* **31** 1733

[9] Chicot G, Pernot J, Santailler JL, Chevalier C, Granier C, Ferret P, Ribeaud A, Feuillet G, and Muret P 2013 *Phys. Stat. Sol. B* **251** 206

[10] Auret FD, Goodman SA, Hayes M, Legodi MJ, van Laarhoven HA and Look DC 2001 *J. Phys. : Condens. Matter* **13** 8989

[11] Auret FD, Wu L, Meyer WE, Nel JM, Legodi MJ and Hayes M 2004 *Phys. Stat. Sol. C* **1** 4

[12] Auret FD, Goodman SA, Legodi MJ, Meyer WE and Look DC 2002 *Appl. Phys. Lett.* **80** 1340

[13] Mtangi W, Auret FD, Nyamhere C, Janse van Rensburg PJ and Chawanda A 2009 *Physica B: Cond. Mat.* **8-11** 1092

[14] Monakhov EV, Kuznetsov AY, Svensson BG 2009 *J. Phys. D: Appl. Phys.* **15** 153001

[15] Scheffler L, Kolkovsky VI, Lavrov EV, and WeberJ 2011 *J. Phys. : Condens. Matter* **23** 334208

[16] Ye ZR, Lu XH, Ding GW, Fung S, Ling CC, Brauer G and Anwand W 2011 *Semicond. Sci. Technol.* **26**095016

[17] Fang ZQ, Claflin B, Look DC, Dong YF, Mosbacker HL and Brillson LJ 2008 *J. Appl. Phys.* **104** 063707

[18] Schifano R, Monakhov EV, Svensson BG, W. Mtangi, van Rensburg PJ, and Auret FD 2009 *Physica B* **404** 4344

[19] Dong Y, Fang ZQ, Look DC, Doutt DR, Cantwell G, Zhang J, Song JJ and Brillson LJ 2010 *J. Appl. Phys.* **108** 103718

[20] Vines L, Monakhov E, Schifano R, Mtangi W, Auret FD, and Svensson BG 2010 *J. Appl. Phys.* **107**103707

[21] Quemener V, Vines L, Monakhov EV, and Svensson BG 2011 *Appl. Phys. Lett.* **99** 112112

[22] Fang ZQ, Claflin B, Look DC, Dong YF and Brillson L 2009 *J. Vac. Sci. Technol. B* **27** 1774

[23] Schröter W, Kronewitz J, Gnauert U, Riedel F, and Seibt M, 1995 Phys. Rev. B **52** 13726.

[24] Watkins GD and Troxell JR 1980 *Phys. Rev. Lett.* **44** 593

[25] Son NT, Trinh XT, Lovlie LS, Svensson BG, Kawahara K, Suda J, Kimoto T, Umeda T, Isoya J, Makino T, Ohshima T, and Janzén E 2012 *Phys. Rev. Lett.* **109** 187603

[26] Thurmond CD 1975 *J. Electrochem. Soc.* **122** 1133

[27] O'Donnell KP and Chen X 1975 *Appl. Phys. Lett.* **58** 2924

[28] Rai RC, Guminiak M, Wilser S, Cai B and Nakarmi ML 2012 *J. Appl. Phys.* **111** 073511

[29] Pässler R 1976 *Phys. Status Solidi B* **78** 625 (1976) and 1978 *Phys. Status Solidi B* **85** 203

[30] Ridley BK 1978 *J. Phys. C : Solid State Phys.* **11** 2323 and 1978 *Solid State Electron.* **21**1319

[31] Henry CH and Lang DV 1977 *Phys. Rev. B* **15** 989

[32] Pässler R 1980 *J. Phys. C : Solid State Phys.* **13** L901

[33] Bourgoin J and Lannoo M 1983 *Point defects in Semiconductors II* , Springer Series in Solid State Science vol. 35, Springer-Verlag, Berlin

[34] Brousseau M 1988 *Les défauts dans les semiconducteurs*, Les Éditions de Physique, Les Ulis, France chap. IV, VII, VIII, IX.

[35] Goguenheim D and Lannoo M 1990 *J. Appl. Phys.* **68** 1059

[36] The numerical simulations showed that the thermal activation of the cross section, involved in the $F(\hbar\omega_q/kT, p_i, S_i)\ C_Z$ factor, can be neglected in comparison with the activation energy E_{an} measured in this work considering phonon energy at 40 meV.

[37] Hofmann DM, Pfisterer D, Sann J, Meyer BK, Tena-Zaera R, Munoz-SanJose V, Frank T, Pensl G 2007 *Appl. Phys.* **A 88** 147

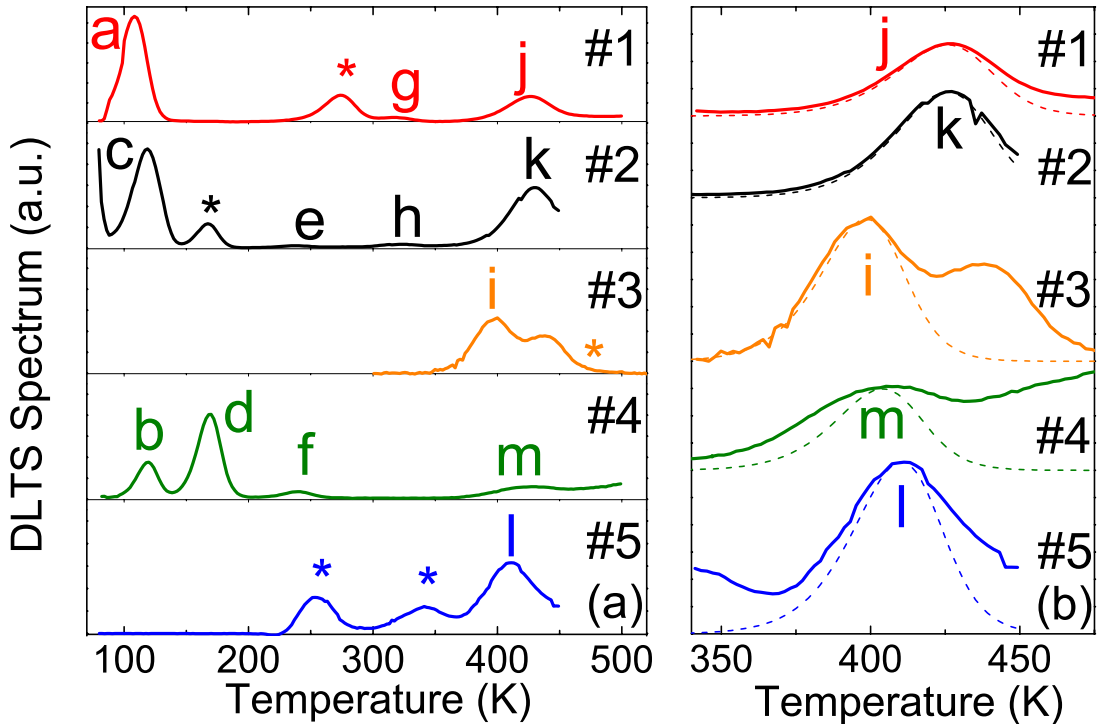

FIG. 1. (a) DLTS spectra for each of the five ZnO samples with label of studied peak (peak labeled with star are not studied in this work). Time windows of 100ms for DLTS spectra of samples #1, #2, 50ms for samples #4, 0.5s for sample #5 and 1s for sample #3 were used on the spectra represented here. (b) [E1000] experimental (full line) and simulated (broken line) spectra, the later being calculated with parameters deduced from Arrhenius fit.

nn,

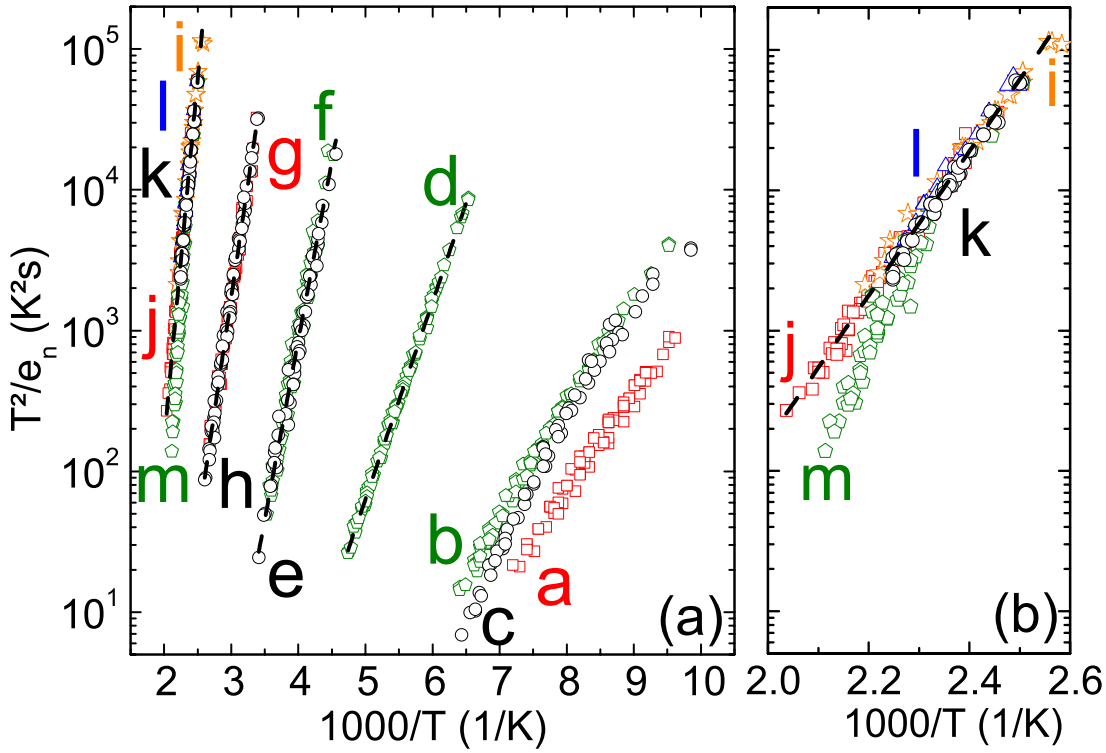

FIG. 2. (a) Arrhenius diagram of levels measured by Fourier transform deep level transient spectroscopy in five $n-$type ZnO samples. A letter label is attributed to each level. (b) Same as (a) but focused on the [E1000] level. Data coming from sample #1 are represented in open squares, #2 in open circles, #3 in open stars, #4 in open pentagons, #5 in open triangles and dash lines correspond to the linear fit of data.

Sample	Growth method/Origin	Remark	$N_d - N_a$ (cm^{-3})
#1	CVT on ZnO/Leti-CEA	homoepitaxial	$3.0\times10^{+15}$
#2	CVT on saphir/Leti-CEA	heteroepitaxial	$1.6\times10^{+16}$
#3	HT/Crystec Inc.	no	$1.2\times10^{+16}$
#4	HT/Tokyo Denpa Inc.	no	$3.0\times10^{+16}$
#5	HT/Tokyo Denpa Inc.	implanted	$2.3\times10^{+16}$

TABLE I. Description of the five samples investigated in the work (growth method, origin of the sample, additional remarks and effective doping $N_d - N_a$ evaluated from C(V) measurement).

Trap	Label	E_{an} (eV)	σ_n (cm^2)	Samples
[E280]	d	0.278 ± 0.001	$1.8 \pm 0.2 \times 10^{-16}$	#4
[E500]	e ,f	0.505 ± 0.006	$2.5 \pm 0.8 \times 10^{-14}$	#2, #4
[E640]	g, h	0.644 ± 0.005	$4.6 \pm 0.9 \times 10^{-15}$	#1, #2
[E1000]	i, j, k, l, m	1.018 ± 0.037	$1.6 \pm 0.4 \times 10^{-13}$	#3, #1, #2, #5, #4

TABLE II. Activation energy (E_{an}) and capture cross section (σ_n) of electron traps detected in the five different ZnO samples investigated in this work. The labels correspond to the ones of the Arrhenius diagram and DLTS spectra.

Samples	N_t (cm^{-3})	W_p(nm)	W_r(nm)
#1	2.6×10^{14}	750	900
#2	4.2×10^{14}	300	470
#3	6.4×10^{14}	440	460
#4	1.2×10^{14}	450	500
#5	3.6×10^{15}	330	450

TABLE III. [E1000] trap density N_t deduced from the capacitance transient amplitude measured by deep level transient spectroscopy, combined to $N_d - N_a$ density from C(V), in the five ZnO samples and averaged on a depth ranging from the space charge region W_p (during pulse voltage U_p) to the space charge region W_r (after the pulse bias and under reverse bias U_r).